

gime⁶ gave $1/H$ behavior in good agreement with experiments on $AuFe$.¹⁰ This result could be physically understood by noting that the thermopower involves the derivative of the lifetime, proportional to $1/H$ in high fields, while the magnetoresistivity and the Hall coefficient involve the lifetimes themselves, giving $\ln H$ behavior.

We can conclude from this study that although the experiments would be difficult it would be very interesting to get systematic data in high fields and low temperatures (say, $\mu_B H/kT \sim 5, 10, 20$) for the magnetoresistivity, the Hall voltage and the ther-

mopower, together with magnetization measurements. Indeed, while perturbation theory does show that $\ln H$ behavior will occur in the high-field regime for ρ and R , and $1/H$ behavior for S , there is considerable uncertainty about the meaning of the spin-polarization terms which appear for large H , and, specifically, one needs to know how much the impurity magnetization is saturated in these large fields.

The authors would like to thank Dr. H. Suhl, Dr. R. More, Dr. J. Kopp, and Dr. P. Monod for many useful discussions.

*Research supported by the Air Force Office of Scientific Research, U.S. Air Force, Grant No. AF-AFOSR-610-67.

†Present address.

‡Laboratoire Associé au Centre National de la Recherche Scientifique.

¹R. More and H. Suhl, *Phys. Rev. Letters* **20**, 500 (1968).

²M. T. Béal-Monod and R. A. Weiner, *Phys. Rev.* **170**, 552 (1968).

³M. D. Daybell and W. A. Steyert, *Phys. Rev. Letters* **20**, 195 (1968).

⁴M. T. Béal-Monod and R. A. Weiner (unpublished).

⁵R. More, *Solid State Commun.* **7**, 237 (1969).

⁶R. A. Weiner and M. T. Béal-Monod, *Phys. Rev. B* **2**, 2675 (1970).

⁷H. Suhl, *J. Appl. Phys.* **39**, 1294 (1968).

⁸M. D. Daybell, W. P. Pratt, Jr., and W. A. Steyert, *Phys. Rev. Letters* **22**, 401 (1969).

⁹P. Monod (unpublished).

¹⁰R. Berman, J. Kopp, and C. T. Walker, in *Proceedings of the Eleventh International Conference on Low Temperature Physics, St. Andrews, 1968*, edited by J. F. Allen, D. M. Finlayson, and D. M. McCall (University of St. Andrews Printing Department, St. Andrews, Scotland, 1969), p. 1238.

Low-Temperature Transport Properties of Dilute Silver-Manganese Alloys

D. Jha and M. H. Jericho*

*Physics Department, Dalhousie University,
Halifax, Nova Scotia, Canada*

(Received 11 May 1970)

We report measurements of the electrical resistivity between 20 and 0.3 K and the thermal conductivity between 4 and 0.6 K of a number of dilute alloys of manganese dissolved in silver. The nominal concentration range of the alloys is from 0.005- to 1.1-at. % Mn. The electrical-resistivity curves for the more concentrated alloys show a resistance maximum at an anti-ferromagnetic ordering temperature T_{\max} which is a characteristic for this alloy system. At lower temperatures, however, a resistivity that is approximately a linear function of temperature is observed. The Lorenz number for the alloys turns out to be concentration dependent, although the deviations from L_0 , the Sommerfeld value for the Lorenz number, are generally not more than about 4%. The results are interpreted in terms of a phenomenological model based on the classical Kondo theory, together with a Lorentzian distribution of internal magnetic fields that exist at an impurity site.

I. INTRODUCTION

If certain magnetic impurities are dissolved in sufficient quantity in the noble metals, then at a low temperature a minimum followed by a maximum at lower temperatures is generally observed in the electrical resistivity of these alloys.¹⁻³ Well below the maximum, an experiment by McDonald⁴ on Au-Fe seemed to indicate that the resistivity can be-

come a linear function of temperature. This interesting observation made it desirable to us to make low-temperature transport measurements on other noble metals containing magnetic impurities. We report here measurements of the electrical resistivity between 0.3 and 20 K and the thermal conductivity between 0.6 and 4.2 K of a number of silver alloys containing manganese as impurities. Our results confirm the findings by other authors of a

resistance maximum which is approximately concentration dependent. Below the maximum the resistivity curves for the more concentrated alloys show a portion that is a linear function of T with the slope of this section being only a weak function of concentration. The thermal results, furthermore, suggest that the Wiedemann-Franz law does not strictly hold in these alloys, although the Lorenz number does not deviate from L_0 , the Sommerfeld value, by more than about 4%.

A manganese impurity in silver has a magnetic moment corresponding to a spin $S=5/2$. In one attempt⁵ to understand the low-temperature specific heat and the resistance maximum in a system like Ag-Mn, it is assumed that the Ruderman-Kittel-Yosida (RKY) interaction between the impurities leads to an ordering of the impurity moments below a certain temperature. In the Ag-Mn system the ordering is of the antiferromagnetic type. The form of the RKY interaction⁶ between impurities requires, however, that any two moments are strongly correlated only if they are not too far apart, that is, only if they are within some coherence range R_c . Below the ordering temperature, one is therefore considering a frozen-in arrangement of impurity moments with antiferromagnetic ordering within some coherence range R_c , where R_c is concentration dependent. The random arrangement of the impurities then makes the internal magnetic field that exists at a given impurity site a statistical quantity; and transport properties are discussed in terms of a probability distribution $P(g\mu_B H)$ which gives the probability that the magnetic energy of a given impurity due to the internal field H caused by all the other moments will be between $g\mu_B H$ and $g\mu_B \times (H+dH)$, where g is the Lande g factor and μ_B is the Bohr magneton.

No rigorous derivation of $P(g\mu_B H)$ for any system has yet been given. The assumption that the impurity spins are distributed according to an Ising model allowed Marshall⁷ and Klein and Brout⁸ to derive an expression for $P(g\mu_B H)$. The $T=0$ K form of the distribution for Ref. 8 is well approximated by a Lorentzian of the form

$$P(g\mu_B H) = \frac{1}{2 \tan^{-1} 4} \frac{\Delta}{\Delta^2 + (g\mu_B H)^2} \quad \text{for } g\mu_B H < 4\Delta$$

$$= 0 \quad \text{for } g\mu_B H > 4\Delta,$$

where Δ is the width of the distribution and is proportional to the concentration. It is necessary to cut the distribution off at some value of $g\mu_B H$, since otherwise $\langle (g\mu_B H)^2 \rangle$ diverges. The choice of 4Δ is somewhat arbitrary, however.

Harrison and Klein⁵ have used this distribution to calculate the electrical resistivity of a statistical antiferromagnet to second order of the Born approximation. Their calculations reproduce most of the

features of our experimental curves such as a resistance maximum at a temperature which is approximately proportional to the impurity concentration, a linear temperature dependence of resistivity at low temperatures and a relatively weak concentration dependence of the slope of this linear region. A more quantitative comparison of that theory with our resistivity results requires numerical evaluation of a number of complex integrals. Furthermore, the theory has not been extended to cover the somewhat more difficult case of the thermal conductivity. It is for these reasons that we prefer to discuss our results in terms of a simple physical model which enables us to obtain a fairly good qualitative understanding of both the electrical resistivity and the thermal conductivity.

In Sec. II we describe the experimental aspects of this work while the electrical and thermal conductivity results are presented in Sec. III. Our model is introduced in Sec. IV where a comparison of the theoretical ideas with the results is attempted.

II. EXPERIMENTAL DETAILS

A. Alloy Preparation

The starting materials for the alloys were high-purity (99.9999%) Cominco silver and 99.99%-pure manganese supplied by Johnson-Matthey. The alloys were prepared by the successive dilution of a Ag-Mn master alloy containing 3.2-at.% Mn. The accurately weighed quantities of the constituents (pure silver and an alloy material) were placed in a spectroscopically pure graphite crucible which was previously degassed at 1000 °C. The crucible was located in a similarly degassed quartz tube filled to a pressure of 1 atm of pure helium after being evacuated to a pressure of less than 10^{-6} Torr. An induction furnace was used to melt the constituents in the crucible, and each melt was given three minutes to homogenize before the power was turned off. Electron-beam microprobe analysis, as well as resistivity measurements on materials obtained from different parts of the same alloy ingot, showed that the alloys were homogeneous.

The ingots were rolled into thin strips approximately 0.2 mm thick. After each rolling step the strips were etched with a dilute nitric acid solution. They were then shaped with a spark-cutting machine into a rectangular shape about 10 cm long and 2×0.2 mm in cross section. The spark cutting was done in such a way that on one side of the sample, two narrow (<0.5 mm in width) fingers of silver alloy separated by about 4.5 cm remained. These acted as the potential and thermal probes. Before mounting in the cryostat, all samples were annealed at 700 °C for 24 h in high vacuum. At this temperature the vapor pressure of Mn should be sufficiently low so that loss of Mn during the heat treatment should not

be very serious. This is confirmed by the proportionality of the low-temperature resistivity to the nominal manganese concentration for the more concentrated alloys.

B. Measurement Techniques

The electrical and thermal conductivities of the samples were measured in a He³ cryostat. The cryostat (except for the magnetic thermometer) is similar in design to that described in Ref. 9. As the samples were very thin, they were supported by two sets of crossed wires mounted inside a rigid stainless-steel frame. The total thermal resistance of the crossed-wire support was at least 10³ times bigger than that of the samples, and therefore the heat leak through the support was negligible.

The thermal conductivity was measured by the steady-state method using a pair of 10-Ω $\frac{1}{10}$ -W Allen Bradley resistors as thermometers. The thermometers were attached to the fingers on the sample described before with Bi-Cd nonsuperconducting solder. To the same pair of probes were also soldered the potential leads for the electrical-resistivity measurement. Thus the same geometrical factor could be used for the calculation of the thermal and electrical conductivities. Between 4.2 and 0.8 K the thermometers were calibrated against the vapor pressures of He⁴ and He³ using the 1958 He⁴ and 1962 He³ temperature scales. Temperatures below 0.6 K were obtained by extrapolating a plot of $\ln R$ vs $\ln P$ ($P = \text{He}^3$ vapor pressure) to lower pressures, and then using the 1962 He³ temperature scale to determine the temperature for the observed resistance values of the carbon thermometers. The procedure should be sufficiently accurate for our purposes. Temperatures above 4.2 K were measured with a calibrated Germanium thermometer. Three calibration points were used for each carbon thermometer to calculate the three constants a_{-1} , a_0 , and a_{+1} in the Clement-Quinnell¹⁰ equation

$$1/T^* = a_{-1}/\ln R + a_0 + a_{+1}\ln R,$$

and a correction curve ($T^* - T$) vs T^* was used for interpolation. In this way the temperatures could be measured correct to a fraction of 1 mK. For the thermal measurements the heat input was adjusted such that a temperature difference ΔT of 200 mK at 4 K and about 60 mK at the lowest temperatures was obtained.

A four-probe arrangement was used to measure the electrical resistivity. The current passed through the samples was limited to a maximum of 50 mA. The voltages were measured using the technique of phase-sensitive detection with a relay modulator in the He⁴ bath as described by Jericho and March.¹¹ To satisfy the low-impedance requirement of the modulator circuit and also to minimize the heat leak, a pair of Nb_{0.75}Zr_{0.25} superconducting

wires (0.003 in. diam) were used as potential leads. The voltage across the sample was compared with the voltage on a reference resistor in the He⁴ bath. Any voltage difference was chopped at a frequency of 80 cps using a DPDT Micro-Scan relay (Model No. C-2350, James Electronics Inc., Chicago). The technique of phase-sensitive detection was then used to obtain the null point. The minimum detectable voltage was 10⁻⁹ V and the potential difference across the samples was measured with an accuracy of about 0.3%.

The largest error in the absolute values of the electrical and thermal conductivities arises from the sample-shape factor determination. The thickness of the sample was measured with a micrometer and the width and the distance between the two probes with a traveling microscope. The total estimated error in the determination of the shape factor was 2%. However, since the same shape factor enters in both the electrical and thermal conductivities it should not affect the Lorenz parameter. The overall accuracy in the measurement of the Lorenz parameter is estimated to be about 1 to 1.5%. Measurements of the electrical and thermal conductivities of one Ag + In¹² as well as one Cu + Ag alloy gave the Sommerfeld value of the Lorenz number within the experimental error.

III. RESULTS

A. Electrical Resistivity

The electrical resistivity of the alloys is shown in Figs. 1-3. The most dilute samples, such as Nos. 5 and 6, show a resistance minimum near 7 K. For lower temperatures the resistivity rises and soon follows a $\ln T$ temperature dependence which goes all the way down to 0.3 K for alloy No. 6. As the Mn concentration is increased a maximum as well as a minimum in the resistivity is observed. This general behavior of the electrical resistivity was already seen by Malms and Woods² for Ag-Mn alloys, and this aspect of the resistivity variation is similar to the behavior of the Cu-Mn, ³ Cd-Mn, and Zn-Mn systems.¹³ As the temperature is decreased sufficiently below the temperature of the maximum, a new feature appears, however. The resistivity becomes an approximately linear function of the temperature and the higher the concentration the wider the temperature range over which the resistivity is a linear function of T (Fig. 2). For the three most concentrated alloys, the slopes of the linear regions as well as the resistivity values at $T = 0$ K obtained by linear extrapolation of the straight lines are given in Table I. The slopes seem to have only a relatively weak concentration dependence while the intercepts are proportional to the concentration. Also recorded in Table I are the temperatures of the observed resistance maxima and minima for the alloys. T_{\max} seems to be approximately pro-

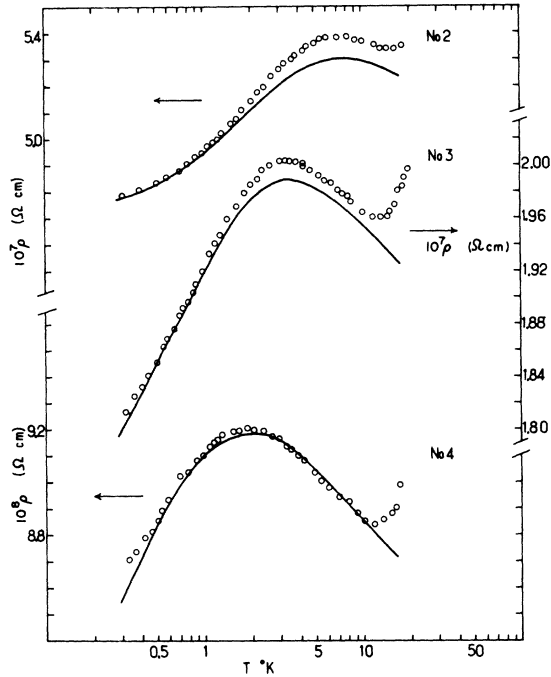


FIG. 1. Electrical resistivity as function of temperature for alloys Nos. 2–4. The solid curves represent the theoretical results according to Eq. (7). Addition of the ideal electrical resistivity to Eq. (7) will produce the resistance minima as well.

portional to the Mn concentration.

The electrical resistivity of a 99.9999%-pure Cominco silver sample was found by Fenton *et al.*¹⁴ to be described by the equation

$$\rho = 6.64 \times 10^{-9} + 2.0 \times 10^{-13} T^{3.5} \quad \text{for } T > 16 \text{ K},$$

where the second term represents the ideal electrical resistivity. In alloys Nos. 5 and 6, we can remove the resistance minimum and thus extend the region where the resistivity is proportional to $\ln T$ if we let the ideal resistivity $\rho_1 = 1.0 \times 10^{-13} T^{3.5}$, which is half the value quoted above. This same expression for ρ_1 also removes the resistance minimum for alloy No. 4 but removes the minimum only partially for alloy No. 3 (possibly due to a breakdown of Matthiessen's rule). The resistivity of the linear portion above T_{\max} for alloys Nos. 3 and 4 was then found to have an approximately logarithmic-temperature dependence as well. The small separation between T_{\max} and T_{\min} in alloys Nos. 1 and 2 made an analysis of this type impossible for these samples.

The resistivity of alloy Nos. 5 and 6 and of alloys Nos. 3 and 4 far above the resistance maximum can then be represented by the expression

$$\rho(T) = -A \ln T + D,$$

where A and D are independent of temperature.

Representative values of the parameter A are

given in Table I. The error in A is probably quite large for the higher-concentration samples, since the range over which we can follow this logarithmic dependence of resistivity on temperature is rather restricted.

B. Thermal-Conductivity Results

The thermal conductivity of all samples was measured between about 0.6 and 4.2 K. For purposes of analysis we assumed that the total thermal conductivity K could be written in the usual form

$$K = K_e + K_g, \quad (1)$$

where K_e is the conductivity due to the conduction electrons and K_g due to phonons. Of particular interest to us is the study of the effects of magnetic-impurity scattering on the heat conductivity of the conduction electrons. Since the effects that we expect are of a rather small magnitude, an accurate knowledge of K_g seems essential for an accurate determination of K_e from the measurements. In the temperature range of interest here, the phonon mean free path is limited mainly through phonon-electron interactions. No theoretical estimate of this interaction is sufficiently precise, however, to permit an accurate determination of K_e . We have therefore assumed that the phonon-electron inter-

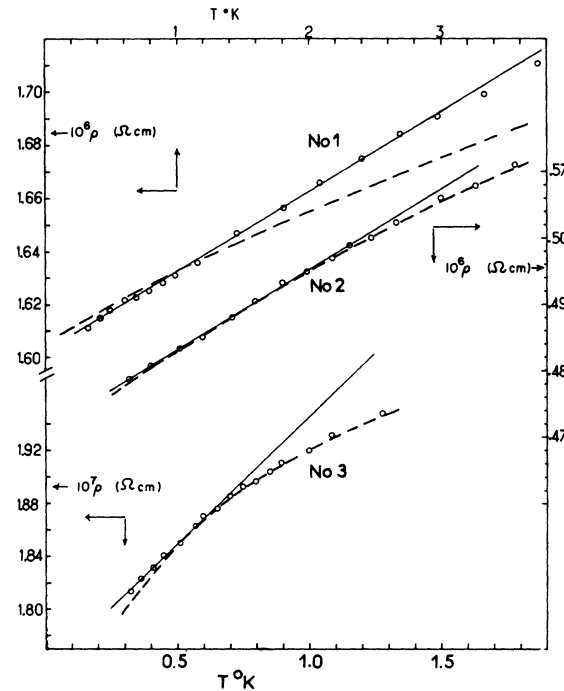


FIG. 2. Electrical resistivity as function of temperature for alloy No. 1 and the low-temperature results for alloys Nos. 2 and 3. The straight solid lines were drawn through the linear temperature-dependent part of the resistivity curves. The dashed lines are the theoretical results according to Eq. (7).

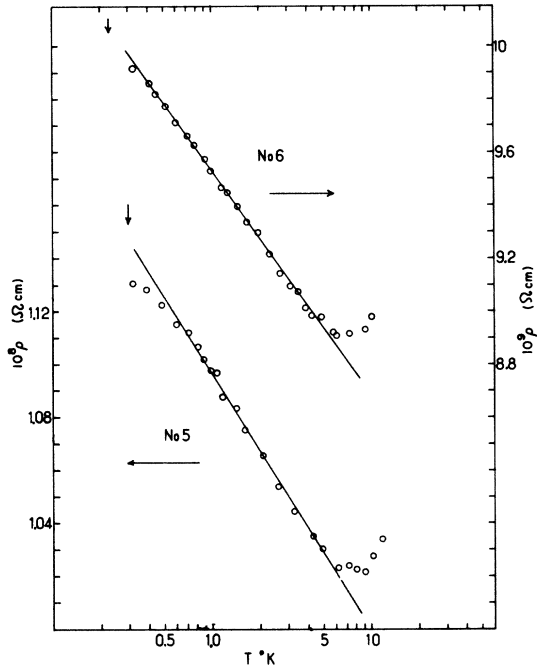


FIG. 3. Electrical resistivity as function of temperature for the two most dilute alloys. Vertical arrows mark the positions of the resistance maxima according to Eq. (7).

action in silver containing magnetic impurities is essentially the same as that in silver containing ordinary impurities; and we have then used available lattice-conductivity data for nonmagnetic silver alloys to obtain an estimate of K_g in our Ag-Mn system. A least-mean-square fit to available data¹⁵ in the resistivity range of our samples suggests that

$$K_g = 7.4 \times 10^{-5} (T^{2.2}/\rho^{0.2}) \text{ W cm}^{-1} \text{ deg}^{-1}. \quad (2)$$

From the magnitude of K_g suggested by this expression we see that K_g is negligible for alloys Nos. 5 and 6 and that a rather large error in K_g can be tolerated for all alloys below 1 K.

If we define a Lorenz parameter L through the expression

$$L = K_g \rho(T) / T,$$

then any deviation from unity of the expression

$$L/L_0 = (K - K_g) \rho(T) / L_0 T \quad (3)$$

can be used as a measure of the breakdown of the Wiedemann-Franz law in our alloy system. In Eq. (3) L_0 is the Sommerfeld value of the Lorenz number and is equal to $2.448 \times 10^{-8} \text{ W cm}^{-1} \text{ deg}^{-2}$. We have calculated L/L_0 for our alloys with the help of Eq. (2) and with the smoothed electrical-resistivity curves shown in Figs. 1–3, and the results are plotted in Fig. 4. We believe that a large portion of the detailed structure that these curves exhibit should not be taken seriously, since many of the features are within the experimental error, but the general trend of having $L/L_0 < 1$ for the concentrated alloys and $L/L_0 > 1$ for the dilute alloys is significant in our opinion. The Lorenz numbers for alloys Nos. 5 and 6 seem to decrease as the temperature is increased. This is not very surprising since for these dilute samples the ideal thermal resistance is not negligible above about 2 K. The thermal resistance due to electron-phonon scattering is expected to be of the form

$$W_i = BT^2.$$

The magnitude of B was taken to be equal to $6 \times 10^{-5} \text{ cm deg}^{-1} \text{ W}^{-1}$, the value used by Van Baarle *et al.*¹⁵ in their lattice-thermal-conductivity calculations for silver. If we correct the results for alloys Nos. 5 and 6 for the ideal thermal resistance in this way we obtain Lorenz numbers for these samples which are constant below 4 K to within our experimental error of about 1.5%.

Neglect of W_i does not affect the results of alloys Nos. 5 and 6 below 1.5 K and has no effect on any of the other alloys below about 4 K. The data points in Fig. 4 for alloy No. 7 are those that were reported before in Ref. 12. These results will be discussed more fully in Sec. IV.

IV. PHENOMENOLOGICAL INTERPRETATION OF RESULTS

The observation that in the very dilute alloys, as well as above the maximum in the more concentrat-

TABLE I. Manganese concentrations and some electrical-resistivity parameters for the alloys.

Alloy No.	Nominal conc. (at. %)	T_{\max} (K)	T_{\min} (K)	Slope of linear region ($n\mu\Omega \text{ cm/K}$)	ρ at $T=0$ K (Extrapol.)		
					A ($n\mu\Omega \text{ cm}$)	a_1	ρ_1 ($\mu\Omega \text{ cm}$)
1	1.12			30.3	1.602		1.605
2	0.332	7.4	15	24	0.47		0.468
3	0.125	3.3	13	20	0.175	5.4	0.1706
4	0.0558	1.9	11.5			3.1	0.0769
5	0.007	<0.3	8			0.44	0.043
6	0.005	<0.3	7			0.38	0.052

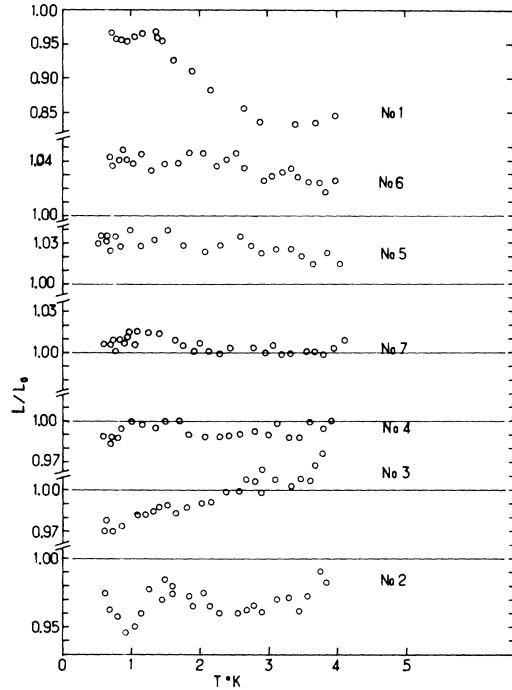


FIG. 4. Temperature dependence of the Lorenz numbers for the alloys. The Lorenz numbers were determined as explained in Sec. III.

ed alloys, the resistivity has a $\ln T$ dependence suggests that we are dealing in these situations with a Kondo type of phenomenon. Below the resistance maximum the Kondo effect thus seems to be inhibited. We can see what might be happening in that region if we briefly consider the classical Kondo effect. In order to obtain a low-temperature resistivity which depends on the temperature, it is necessary to consider conduction-electron scattering by the magnetic impurities in second-order perturbation theory. The second-order terms in the scattering involve the density of available intermediate states. The density of available intermediate states, however, depends on the Fermi function for the conduction electrons so that the electron-scattering time will now depend on temperature. In this model the spin-flip scattering of the conduction electrons by the impurity spins is still an elastic process. The $\ln T$ dependence of ρ thus results from elastic spin-flip scattering of the conduction electrons in second-order perturbation theory. The ordinary Kondo effect should thus be quenched if the impurities are placed in a magnetic field so that the degeneracy of the magnetic-impurity states is removed and spin-flip scattering becomes an inelastic process. We now argue that if the separation of the energy levels of an impurity is $g\mu_B H$ then only those conduction electrons that have a thermal energy $k_B T \gtrsim g\mu_B H$ can flip impurity spins and can thus contribute to the

classical Kondo effect. To discuss the transport properties over the whole temperature range, we assume that the internal field distribution has a Lorentzian form and is given by

$$P(g\mu_B H) = \Delta/\pi[\Delta^2 + (g\mu_B H)^2] . \quad (4)$$

The distribution is symmetric and is shown in Fig. 5. Within a region about the center of width $2k_B T$ we assume we have a Kondo type of behavior for the resistivity,¹⁶ while outside that region we assume that the resistivity is ρ_0 , a constant. For this model to be applicable requires the Kondo temperature to be much lower than the lowest temperature of the resistivity measurements. It is not clear what the actual Kondo temperature of the Ag-Mn system is, but it is probably as low as T_k for the Cu-Mn system, i. e., $T_k < 0.1$ K. The fact that down to 0.3 K no deviation from a $\ln T$ behavior is discernible in our most dilute alloy confirms the belief that T_k is indeed very low for Ag-Mn. The lack of a precise value of T_k makes it even more difficult to decide which form of the resistivity expression to adopt, since the original expression derived by Kondo should, strictly speaking, be valid only when $T > (T_F T_k)^{1/2}$. Thus, instead of relying on any theoretical model we take the phenomenological approach and write the Kondo type of resistivity in the form

$$\rho_k(T) = -\rho_2 \ln T + \rho_3, \quad (5)$$

where ρ_2 and ρ_3 are temperature independent.

The magnetic part of the electrical resistivity is then given by

$$\begin{aligned} \rho_M(T) &= P(g\mu_B H) \rho(T) d(g\mu_B H) \\ &= \frac{2 \Delta \rho_k(T) d(g\mu_B H)}{\pi \Delta^2 + (g\mu_B H)^2} + \frac{2 \Delta \rho_0 d(g\mu_B H)}{\pi \Delta^2 + (g\mu_B H)^2} \\ &= \rho_0 - \frac{2}{\pi} \rho_2 \left(\ln T - \frac{(\rho_3 - \rho_0)}{\rho_2} \right) \tan^{-1} \frac{k_B T}{\Delta} . \end{aligned}$$

To this we must add a resistivity ρ_l which is temperature independent and which represents the con-

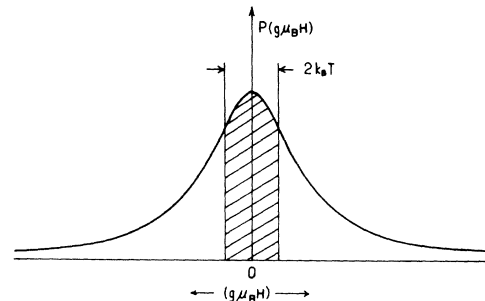


FIG. 5. Lorentzian probability distribution of internal magnetic fields. The Kondo effect is assumed to be quenched for fields outside the shaded region.

tribution from nonmagnetic-potential scattering of the conduction electrons by the impurities. Furthermore, the width of the distribution Δ is proportional to the impurity concentration c so that we can set $k_B T/\Delta = a_2 T/c$. We thus obtain the following expression for the resistivity of our alloys:

$$\rho(T) = \rho_1 \left[1 - (2/\pi) a_1 (\ln T - a_3) \tan^{-1}(a_2 T/c) \right], \quad (6)$$

where $\rho_1 = (\rho_I + \rho_0)$, $a_1 = \rho_2 / (\rho_I + \rho_0)$ and $a_3 = (\rho_3 - \rho_0) / \rho_2$. The resistivity has thus been expressed in terms of a number of parameters which can be determined by comparing Eq. (6) with the experimental results.

It is instructive to consider Eq. (6) in the limits $T/c \gg 1$ and $T/c \ll 1$.

When $T/c \gg 1$, $\tan^{-1}(a_2 T/c) \approx \pi/2$ so that we have

$$\rho(T) = \rho_1 [1 - a_1 (\ln T - a_3)],$$

which is the Kondo type of resistivity that we started from. When $T/c \ll 1$, $\tan^{-1}(a_2 T/c) \approx a_2 T/c$ and we obtain

$$\rho(T) = \rho_1 [1 - (2/\pi) a_1 (\ln T - a_3) a_2 T/c].$$

For the more concentrated alloys the low-temperature resistivity should thus contain a term proportional to $T \ln T$ and a term proportional to T . This is essentially the result of Harrison and Klein.⁵ Furthermore, as $T \rightarrow 0$ K, $\rho(T) \rightarrow \rho_1$.

To compare Eq. (6) with the experimental results, we note first of all that when $T/c \gg 1$ we can determine $\rho_1 a_1$ from a plot of $\rho(T)$ vs $\ln T$. The values for some of the alloys are given under *A* in Table I. If ρ_1 is strictly proportional to the concentration, then we can use the three values of ρ_1 for alloys 1, 2, and 3 obtained by extrapolating the linear resistivity regions to $T=0$ to determine a_1 . The values of a_1 calculated in this way are also given in Table I. The parameter a_1 should be concentration independent. The variation in a_1 suggested by Table I is thus most likely caused by the inability to measure slopes accurately for the concentrated alloys and by the uncertainty of the exact impurity concentration for alloys Nos. 5 and 6. In analyzing the results we have therefore taken an average value and set $a_1 = 0.043$.

The impurity concentrations given in Table I are only nominal values. We have therefore determined ρ_1 by fitting Eq. (6) to the data at $T=1$ K so that if $\rho(1)$ is the experimentally determined resistivity at $T=1$ K we can write

$$\rho(T) = \frac{\rho(1)}{1 + (2/\pi) a_1 a_3 \tan^{-1}(a_2/c)} \times \left[1 - \left(\frac{2}{\pi} \right) a_1 (\ln T - a_3) \tan^{-1} \left(\frac{a_2 T}{c} \right) \right]. \quad (7)$$

At this stage we would like to point out that any given resistivity curve could be fitted extremely well with Eq. (7) if the parameters a_2 and a_3 were adjusted for each alloy separately. These parameters should, however, be the same for each alloy, and a good over-all fit to all the alloys was obtained when $a_2 = 0.12$ and $a_3 = 6.0$.

With this choice of parameters we obtained the solid curves shown in Fig. 1 and the dashed curves in Fig. 2. These curves do not include the ideal electrical resistance. The general agreement is encouraging if we keep the simplicity of the model in mind. It is difficult to quote an error for the parameters a_1 , a_2 , and a_3 . If we fix a_1 and a_2 as above and let $a_3 = 6.7$ instead of 6, we get a very good fit to the data of alloy No. 1 in Fig. 2. We therefore suggest that the values of the parameters are as given above to within 10 or 15%.

With a_1 , a_2 , and a_3 determined we can calculate ρ_1 and these values are given in Table I. The agreement with the values obtained through extrapolation is as good as can be expected. Below the resistance maximum the resistivity is determined mainly by the $\tan^{-1}(a_2 T/c)$ term, so that since ρ_1 is proportional to the concentration of impurities we expect $[\rho(T) - \rho_1] / \rho_1$ to be a function of T/c . If the results are plotted in this way we find indeed that such a relationship is obeyed below the resistance maximum to within 10 to 15%. Our resistivity results thus represent additional evidence for the validity of the reduced diagram representations for statistical antiferromagnets suggested by Tournier and Souletie.⁶

A. Thermal Conductivity

Our main objective in this section is to obtain a qualitative understanding of the temperature and concentration dependence of the Lorenz number of the alloys. We therefore again assume that we can add the reciprocal relaxation times due to various scattering mechanisms, and we furthermore restrict the discussion to a spin $s = \frac{1}{2}$ system.

We can apply the same considerations that we used in the discussion of the electrical resistivity to the thermal resistance. It was shown by Taylor¹² that at least in the situation where the magnetic-scattering problem can be treated in second-order perturbation theory one finds an expression for the thermal resistance quite analogous to Eq. (5). If W_0 is the thermal resistance for the situation when $g \mu_B H > k_B T$ then we can write for the thermal resistance caused by the elastic scattering of the conduction electrons

$$W(T) = W_I + W_0 - \frac{2}{\pi} W_2 \left(\ln T - \frac{(W_3 - W_0)}{W_2} \right) \tan^{-1} \frac{k_B T}{\Delta}. \quad (8)$$

In addition to the elastic scattering we must now also make allowance for the fact that the internal

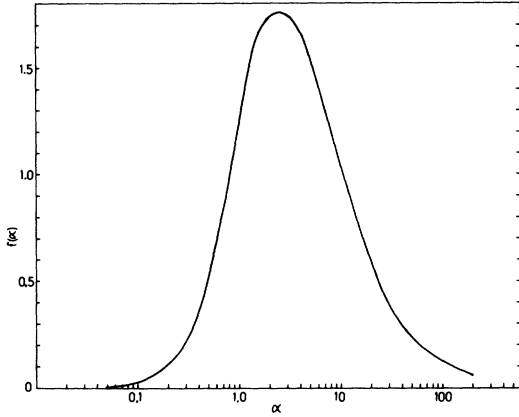


FIG. 6. Variation of the function $f(\alpha)$, defined through Eq. (10), with α .

magnetic fields cause a Zeeman splitting of the impurity states so that inelastic scattering of the conduction electrons is possible. This part of the scattering was neglected in the discussion of the electrical resistivity since only large angle scattering is effective in returning an electron distribution shifted by an electric field back to equilibrium. Inelastic scattering is, however, very effective

The Lorenz number for the alloys is then

$$L = \frac{\rho(T)}{TW(T)} = \frac{\rho_I + \rho_0 - (2/\pi)\rho_2 [\ln T - (\rho_3 - \rho_0)/\rho_2] \tan^{-1}(k_B T/\Delta)}{\{W_I + W_0 - (2/\pi)W_2 [\ln T - (W_3 - W_0)/W_2] \tan^{-1}(k_B T/\Delta) + W_4(T)\} T}$$

Experiment shows that the magnetic effects are small, so that all electrical-resistivity terms are small compared to $\rho_I + \rho_0$ and all thermal-resistivity terms are small compared to $W_I + W_0$. If we retain only first-order terms we can then write

$$\frac{L}{L_0} = 1 + \frac{2}{\pi} \left(\frac{\rho_3}{\rho_1} - \frac{W_3}{W_1} \right) \tan^{-1} \left(\frac{k_B T}{\Delta} \right) - \frac{6}{\pi^2} \frac{\rho_0 \alpha^3}{(\tan^{-1} 4) \rho_1} \int_0^4 \frac{t^3 dt}{(1+t^2) \sinh(\alpha t)}, \quad (11)$$

where $L_0 = \rho_I/TW_1$, $\rho_2/\rho_1 \approx W_2/W_1$, and $\rho_0/\rho_1 = W_0/W_1$.

This expression shows that since Δ is proportional to c and ρ_0'' and ρ_1 are both proportional to c the Lorenz number should be a function of T/c . If we plot the data of Fig. 4 in this way the T/c dependence of the Lorenz number seems to be followed by most samples. The higher-temperature points for alloy Nos. 1 and 4 do not follow this general pattern very well, however. The reason that the high-temperature points of some samples do not

in relaxing a thermally perturbed distribution so that this type of scattering must be considered. An expression for the thermal resistance of a metal where the impurities can exist in two energy states separated by an amount ΔE was given by Ziman,¹⁷ and we adopt his result and write

$$W_4(T, H) = \frac{x}{L_0 T^2 \sinh x} \left[\rho_0' + \frac{3}{\pi^2} x^2 \left(\rho_0'' - \frac{1}{6} \rho_0' \right) \right], \quad (9)$$

where $x = g\mu_B H/k_B T$ and where ρ_0' and ρ_0'' are proportional to c and contain the scattering cross sections. If we are dealing mainly with forward scattering then $\rho_0'' \gg \rho_0'$ so that we can write $W_4(T, H) = 3\rho_0'' x^3 / [2L_0 T (\sinh x) \pi^2]$.

Since we have a distribution of internal fields we must multiply this expression by $P(g\mu_B H)$ and integrate over the fields. If we truncate the distribution at $g\mu_B H = 4\Delta$ then we obtain

$$W_4(T) = \frac{\alpha^3}{L_0 T} R \int_0^4 \frac{t^3 dt}{(1+t^2) \sinh(\alpha t)} = \frac{R}{L_0 T} f(\alpha), \quad (10)$$

where $\alpha = \Delta/k_B T$ and $R = 6\rho_0''/\pi^2 \tan^{-1/4}$.

The integral in Eq. (10) was evaluated numerically, and the variation of the function $f(\alpha)$ with α is shown in Fig. 6. The total thermal resistance is then the sum of Eqs. (8) and (10).

conform to the general trend is most likely caused by an overestimate of the phonon conductivity in these samples. For example, an error in K_ϕ of only 20% could easily bring the high-temperature

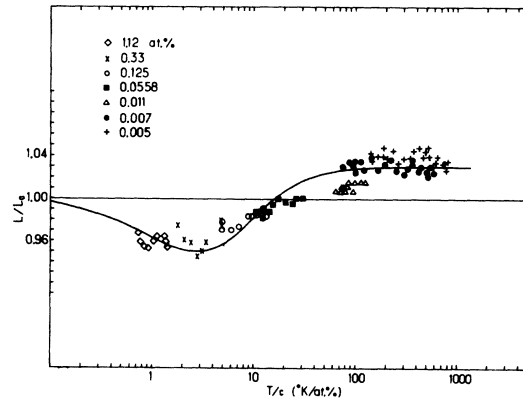


FIG. 7. Lorenz numbers of the alloys below 1.5 K as a function of T/c . The solid curve represents the theoretical result according to Eq. (11).

points of alloy No. 1 in line with the general trend. The data points below about 1.5 K should, however, be essentially unaffected by an error in K_g . Furthermore, it seems unlikely to us that an appreciable lattice conductivity should be present in samples Nos. 5 and 6 even at 4 K. In Fig. 7 we have therefore plotted as a function of T/c the data points below 1.5 K for all the more concentrated alloys, while we plotted all the data points for alloy Nos. 5 and 6. For this plot, the results for alloy Nos. 5 and 6 were corrected for the ideal thermal resistance as discussed in Sec. III. From Fig. 7 we see that L/L_0 does seem to be a function of $1/c$ although the dependence on temperature is less well established. The deviations of the Lorenz number from the Sommerfeld value are never larger than about 4%, however. When T/c is around 2 or 3, the Lorenz number is depressed below L_0 by about 4%, and L approaches a constant value about 3 or 4% above L_0 when $T/c > 10^2$. These observations are in agreement with the predictions of Eq. (11) if we assume that actually a minimum exists in $L(T)/L_0$ when $T/c \approx 2$ or 3. When T/c is small the behavior of $L(T)/L_0$ is dominated by $W_4(T)$, and since this function possesses a maximum we expect a minimum in L/L_0 . When T/c is sufficiently large $W_4(T)$ is negligible, and Eq. (11) predicts a constant value for $[L(T) - L_0]/L_0$ equal to $(\rho_3/\rho_1) - (W_3/W_1)$. Second-order perturbation theory suggests that

$$(\rho_3/\rho_1) - (W_3/W_1) = \frac{2}{3}(\rho_2/\rho_1) = \frac{2}{3}a_1,$$

and thus predicts about a 3% effect, which seems to agree with the experiments. The maximum in $W_4(T)$ occurs at $\alpha = 2.75$. Then if we let $a_2 = 0.12$, the value that was determined from the resistivity curves, we expect a minimum in L/L_0 when $T/c \approx 3$ which is not inconsistent with the experimental results. Whether a minimum actually does exist near $T/c \approx 3$ can only be decided, however, through further thermal measurements on a 1% Mn alloy to much lower temperatures.

If we use in Eq. (11) the values of a_1 and a_2 that were determined from the electrical-resistivity curves and determine ρ_0''/ρ_1 by taking $L/L_0 = 0.95$ at the minimum we obtain the solid curve in Fig. 7. The agreement is perhaps as good as can be expected in view of the various assumptions made.

V. DISCUSSION

The simple physical model that we introduced seems to give a fairly good qualitative explanation of the electrical resistivity and perhaps also of the thermal conductivity of the silver-manganese alloy system. If we use Eq. (7) to determine the expected positions for the maxima in the resistivity curves for alloys Nos. 5 and 6 we find $T_M = 0.298$ K for No. 5 and $T_M = 0.225$ K for No. 6. These values are indicated by arrows in Fig. 3. We see that for alloy No. 5 the

lowest-temperature points seem to fall below the straight line that represents the $\ln T$ dependence of ρ , and a T_M of ~ 0.3 K is not impossible. It would be very interesting to continue such measurements to lower temperatures to see when the present model does break down as it inevitably has to.

It might now be supposed that the success of the model in explaining most of the characteristic features of the electrical and thermal conductivity implies that the probability distribution for the internal fields must be a Lorentzian. This we think, however, is not the case. For example, the temperature at which the resistance is maximum is approximately proportional to the concentration, but that result should follow as soon as we assume that the width of the distribution is proportional to c , and the small field probability is proportional to $1/c$.

Furthermore, the approximately linear temperature dependence of the resistivity at low temperature simply suggests that in a range $k_B T$, corresponding to the temperature range of the linear resistivity region, the probability distribution varies slowly with field. A Lorentzian distribution can satisfy all these requirements, but our experiments, which are limited to temperatures above 0.3 K, do not enable us to distinguish between the Lorentzian distribution of Fig. 5 or a distribution of the type shown in Fig. 8 where the width of the "hole" near $g\mu_B H \approx 0$ is of the order of $0.2k_B$ for our most concentrated alloy.

The predictions of the model in the thermal-conductivity case are perhaps less well confirmed by the experiments, due both to the much larger experimental error in the thermal-conductivity measurements and to the difficulty in separating the various transport terms. Nevertheless, it is interesting to note that the fit to the data shown in Fig. 7 was obtained by the adjustment of only one parameter, ρ_0''/ρ_1 . As in the electrical-resistivity case, further measurements to much lower temperatures are highly desirable.

In connection with our thermal-conductivity results, we would like to mention the results of Spohr and Webber¹⁸ on one Mg-Mn alloy and one Mg-Fe

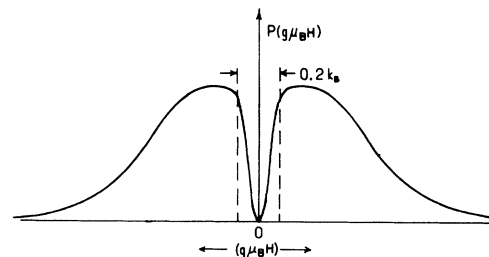


FIG. 8. Another possible model for the probability distribution of internal fields.

alloy. Their electrical-resistivity results on these samples can be put in the form of the high-temperature limit of Eq. (6) with a $\alpha_1 \approx 0.09$ for Mg-Mn and $\alpha_1 \approx 0.02$ for Mg-Fe. The predicted values of $L/L_0 = 1.06$ and 1.01 , respectively, are in close agreement with the experimentally observed values of 1.08 for Mg-Mn and 1.02 for Mg-Fe.

VI. SUMMARY

The most interesting aspect of our resistivity results is the approximately linear temperature dependence of the resistivity below the resistance maximum for the more concentrated alloys. In that respect the Ag-Mn system behaves similarly to the Au-Fe system investigated by McDonald.⁴ The assumption that internal magnetic fields at an impurity site are given by a Lorentzian distribution together with the assumption that the conduction electrons can undergo a Kondo type of scattering only when the local magnetic field $H < k_B T / g \mu_B$, where $k_B T$ is the thermal smearing of the Fermi surface, enable us to derive a phenomenological expression for the electrical resistivity which described the experimental results surprisingly well.

Thermal-conductivity measurements on the same alloy series enabled us to determine Lorenz numbers for the alloys. Because of the difficulty of obtaining an accurate estimate of the phonon heat conductivity the results for the more concentrated alloys above about 1.5 K should be considered with caution. Below this temperature the results are thought to be free from errors caused by separation

of the various transport terms. The Lorenz number was then found to be 3 to 4% above L_0 , the Sommerfeld value, for very dilute alloys and about 4% below L_0 for the most concentrated samples. The positive deviation for the dilute samples seems to agree with a perturbation calculation for the Lorenz number due to Taylor,^{1,2} while the negative deviation was interpreted to be caused by inelastic electron scattering due to the Zeeman splitting of the impurity states.

Our interpretation of the resistivity results was done entirely on a phenomenological basis in terms of a three-parameter expression. The uncertainty in the correct value of the Kondo temperature for the Ag-Mn system makes it difficult to decide which theoretical resistivity expression one should adopt above the resistance maximum, and we have therefore not attempted to relate our three parameters to more fundamental quantities such as the exchange energy J .

ACKNOWLEDGMENTS

We gratefully acknowledge many very valuable discussions concerning the interpretation of the results with Dr. J. Souletie, Dr. K. Matho, and Dr. P. L. Taylor. One of us (M. H. J.) would like to thank Professor Dreyfus for making it possible to spend part of a sabbatical year at CNRS in Grenoble, and furthermore gratefully acknowledges the receipt of a Senior Exchange Fellowship from the National Research Council of Canada.

*Work supported by grants from the National Research Council of Canada.

¹A. N. Gerritsen and J. O. Linde, *Physica* **17**, 573 (1951).

²H. L. Malm and S. B. Woods, *Can. J. Phys.* **44**, 2293 (1966).

³R. W. Schmitt and I. S. Jacobs, *J. Phys. Chem. Solids* **3**, 324 (1957); A. Nakamura and N. Kinoshita, *J. Phys. Soc. Japan* **27**, 382 (1969).

⁴D. K. C. McDonald, W. B. Pearson, and I. M. Templeton, *Proc. Roy. Soc. (London)* **A266**, 161 (1962).

⁵R. J. Harrison and M. W. Klein, *Phys. Rev.* **154**, 540 (1967). The molecular-field model was first applied to the alloy problem by A. Blandin, *J. Phys. Radium* **20**, 160 (1959). The prediction of a low-temperature resistivity increase which is linear in T and independent of concentration was first made by M. T. Beal, *J. Phys. Chem. Solids* **25**, 543 (1964).

⁶A discussion of the consequences of the geometric characteristics of the RKY interaction is given by J. Souletie and R. Tourmier, *J. Low Temp. Phys.* **1**, 95 (1969).

⁷W. Marshall, *Phys. Rev.* **118**, 1519 (1960).

⁸M. W. Klein and R. Brout, *Phys. Rev.* **132**, 2412 (1963).

⁹M. A. Archibald, J. E. Dunick, and M. H. Jericho, *Phys. Rev.* **153**, 786 (1967).

¹⁰J. R. Clement and E. H. Quinell, *Rev. Sci. Instr.* **23**, 213 (1952).

¹¹M. H. Jericho and R. H. March, *Rev. Sci. Instr.* **38**, 428 (1967).

¹²D. Jha, M. H. Jericho, and P. L. Taylor, *Phys. Rev.* **1**, 1870 (1970).

¹³F. Hedgcock and C. Rizzuto, *Phys. Rev.* **163**, 517 (1967).

¹⁴E. W. Fenton, J. S. Rogers, and S. B. Woods, *Can. J. Phys.* **41**, 2026 (1963).

¹⁵C. Van Baarle, F. W. Gorter, and P. Winsemius, *Physica* **35**, 223 (1967).

¹⁶A similar model was independently suggested by J. Souletie.

¹⁷J. H. Ziman, *Electrons and Phonons* (Clarendon, Oxford, England, 1960).

¹⁸D. A. Spohr and R. T. Webber, *Phys. Rev.* **105**, 1427 (1957).